

# Cation-induced structural variations in the alkali metal derivatives of 2-trimethylsilylamino-pyridine: synthesis and X-ray structures of complexes for all five metals Li–Cs with 12-crown-4†

Stephen T. Liddle and William Clegg\*

Department of Chemistry, Bedson Building, University of Newcastle upon Tyne, Newcastle upon Tyne, UK NE1 7RU. E-mail: w.clegg@ncl.ac.uk

Received 3rd November 2000, Accepted 22nd December 2000

First published as an Advance Article on the web 29th January 2001

The secondary amine 2-trimethylsilylamino-pyridine [PyN(H)SiMe<sub>3</sub>] **1** was synthesised by mono-lithiation of 2-aminopyridine and subsequent reaction with Me<sub>3</sub>SiCl. The compound is readily metallated by Bu<sup>n</sup>Li in ethereal solvent, in the presence of the macrocyclic polyether 12-crown-4 (12C4), to afford the lithium secondary amide complex [Li(PyNSiMe<sub>3</sub>)(12C4)] **2**, in which the amide ligand binds through both the amido and pyridyl nitrogen centres. Metathesis of **2** with Bu<sup>t</sup>ONa yields the unusual ‘ate’ solvent-separated ion pair complex [Na(12C4)<sub>2</sub>]-[Na(PyNSiMe<sub>3</sub>)<sub>2</sub>(THF)]·(THF) **3**. Metathesis of **2** with ROM [R = Bu<sup>t</sup>, M = K; R = CH<sub>3</sub>CH<sub>2</sub>CH<sub>2</sub>CH<sub>2</sub>C(CH<sub>2</sub>-CH<sub>3</sub>)HCH<sub>2</sub>, M = Rb] yields the two bridged dimers [{K(PyNSiMe<sub>3</sub>)(12C4)}<sub>2</sub>]·2PhMe **4** and [{Rb(PyNSiMe<sub>3</sub>)(12C4)}<sub>2</sub>]·2PhMe **5**. In both **4** and **5** the amido and pyridyl nitrogens bridge between metal centres. Room temperature metathesis of **2** with CH<sub>3</sub>CH<sub>2</sub>CH<sub>2</sub>CH<sub>2</sub>C(CH<sub>2</sub>CH<sub>3</sub>)HCH<sub>2</sub>OCs yields the polymeric [{Cs(PyNH)(12C4)}<sub>∞</sub>] **6** containing tetranuclear cluster units, with concomitant cleavage of the N–Si bond. Such cleavage is prevented by low temperature synthesis, yielding the bridged dimer complex [{Cs(PyNSiMe<sub>3</sub>)(12C4)}<sub>2</sub>]·PhMe **7**. The compounds have been characterised by multinuclear NMR spectroscopy, CHN microanalysis and (for **2–7**) X-ray crystallography.

## Introduction

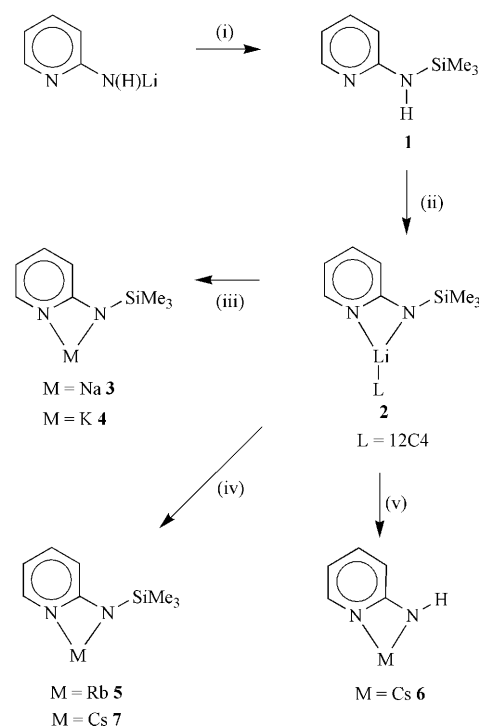
The past two decades have seen enormous interest in the structure and reactivity of alkali metal derivatives of alkyls, alkoxides, imides and amides.<sup>1–6</sup> The widespread synthetic utility of these reagents has led to structural investigations of simple systems revealing a wide range of trends ranging from monomers to polymeric species. However, whilst lithium amides have received much attention, the chemistry of the heavier alkali metal analogues still remains relatively unexplored.<sup>7</sup> Since the bonding is primarily ionic in nature, the structures adopted are highly dependent upon the electronic and steric properties of the substituents at the donor centre and the presence of co-ligands such as tetrahydrofuran (THF), *N,N,N',N'*-tetramethylethylenediamine (TMEDA), and hexamethylphosphoramide (HMPA). Given that the coordination of additional donor ligands to alkali metals greatly improves their reactivity by reducing the extent of aggregation, we became interested in combining alkali metal amides with matched or mismatched crown ethers to investigate the structural consequences a multidentate crown would have for the state of aggregation and the solid state structures adopted. Here we report the synthesis of the secondary amine 2-trimethylsilylamino-pyridine and the preparation and structures of the corresponding lithium, sodium, potassium, rubidium and caesium amides with 12-crown-4 (12C4).

## Results and discussion

### Synthesis and characterisation of compounds 1–7

Treatment of 2-aminopyridine with one equivalent of Bu<sup>n</sup>Li

yields the lithiated primary amide, which, upon addition of chlorotrimethylsilane and elimination of lithium chloride, yields the secondary amine 2-trimethylsilylamino-pyridine [PyN(H)SiMe<sub>3</sub>] **1** as a viscous, colourless oil in excellent yield (Scheme 1). Its <sup>1</sup>H and <sup>13</sup>C NMR spectra exhibit the expected



**Scheme 1** Reagents and conditions: (i) Et<sub>2</sub>O, Me<sub>3</sub>SiCl, 0 °C, (ii) THF, Bu<sup>n</sup>Li, 12C4, (iii) THF, Bu<sup>t</sup>OM (M = Na or K), (iv) THF, CH<sub>3</sub>CH<sub>2</sub>-CH<sub>2</sub>CH<sub>2</sub>C(CH<sub>2</sub>CH<sub>3</sub>)HCH<sub>2</sub>OM (M = Rb or Cs) –78 °C, (v) THF, CH<sub>3</sub>CH<sub>2</sub>CH<sub>2</sub>CH<sub>2</sub>C(CH<sub>2</sub>CH<sub>3</sub>)HCH<sub>2</sub>OCs (M = Rb or Cs).

† Dedicated to the affectionate memory of Ron Snaith, a valued collaborator, friend and verbal sparring partner, who made structural alkali metal chemistry a major part of my research through joint projects beginning in 1983, enriching and promoting our respective careers.

signals and the  $^{29}\text{Si}$  NMR spectrum consists of a single peak at 2.43 ppm, consistent with the chemical shift Raston and co-workers reported for the ligand 6-methyl-2-trimethylsilylaminopyridine.<sup>8</sup>

Treatment of 2-trimethylsilylaminopyridine **1** with one equivalent of  $\text{Bu}^n\text{Li}$  in THF in the presence of 12-crown-4 ether and removal of volatiles *in vacuo* yields a dark red oil, and ultimately crystalline **2** after recrystallisation from methylcyclohexane–THF. The product exhibits appropriate signals in its  $^1\text{H}$  and  $^{13}\text{C}$  NMR spectra. The  $^{29}\text{Si}$  NMR spectrum consists of a single peak at  $-13.38$  ppm, which is a considerable shift upfield from the parent amine **1**, reflecting the increased shielding at the amide centre that might be expected when coordinated to a lithium centre.

With the exception of **6**, we find that metathesis of **2** with a heavier alkali metal alkoxide is successful and yields the desired products in essentially quantitative yields (Scheme 1). Although the reactions are reminiscent of superbasic mixtures, **2–7** crystallise as the desired homometallic complexes. This is perhaps not surprising, since superbases are notoriously difficult to crystallise and the lithium alkoxide side products are extremely soluble, even in hydrocarbon solvents. In all instances the  $^1\text{H}$  and  $^{13}\text{C}$  NMR spectra exhibit the appropriate signals. The  $^{29}\text{Si}$  NMR spectra exhibit a progressive upfield shift on moving down the group [ $-17.40$  (Na),  $-17.39$  (K),  $-17.87$  (Rb) and  $-18.22$  ppm (Cs)] in keeping with the trend of increased shielding at the amido centre by heavier, more polarisable metal centres. Assuming the solid state structures persist in solution, the chemical shifts can be tentatively rationalised by the solid state structures. The essentially identical shifts of **3** and **4** are attributed to the increased shielding effect of the softer potassium being balanced by the bridging nature of the ligand observed in the solid state. The progressive upfield shift from **4** observed in **5** and **7** is proposed to be a direct result of the change in cation, as the core of each structure is a bridged dimer.

Metathesis of **2** with caesium 2-ethylhexoxide at room temperature leads to a N–Si bond cleavage reaction to generate the primary amide complex **6**. The loss of the trimethylsilyl group is clearly apparent in the  $^1\text{H}$  and  $^{13}\text{C}$  NMR spectra and the complex is  $^{29}\text{Si}$  silent. The cleavage of the N–Si bond and formation of a primary amide is confirmed by a sharp peak at 3.79 ppm attributed to the N–H protons. The  $^{133}\text{Cs}$  NMR spectrum exhibits a signal at 29.84 ppm, the broad appearance of which implies that the tetranuclear core or fragments of the polymer may be retained in solution. We speculate that a lithiated silylether is concomitantly formed and further studies are currently underway to isolate and identify all products. However, we find that, if addition of the caesium alkoxides is carried out dropwise at  $-78$  °C, then N–Si cleavage is prevented and the silylated complex is readily obtained, as confirmed by the expected signals in the  $^1\text{H}$ ,  $^{13}\text{C}$  and  $^{29}\text{Si}$  NMR spectra. The  $^{133}\text{Cs}$  NMR spectrum exhibits a sharp signal at 51.40 ppm, a considerable shift downfield from **6**, attributed to the different electronic environments of the two amides.

### Solid state structures of compounds 2–7

The structure of **2** is shown in Fig. 1, and selected bond lengths are listed in Table 1. The complex crystallises as discrete monomers with no particular intermolecular interactions. Lithium is six-coordinate with a short Li(1)–N(2) bond [2.057(2) Å] and a longer Li(1)–N(1) bond [2.203(2) Å] forming a natural bite angle of 64.96(7)°. The Li(1)–N(2) bond length is in good agreement with those reported in the complexes  $[\text{Li}\{\text{N}(\text{Py}-6\text{-Me})(\text{SiMe}_3)\}_2(\text{TMEDA})]$ <sup>8</sup> and  $[\text{Li}\{\text{N}(\text{SiMe}_2\text{Ph})_2\}_2(12\text{C}4)]$ .<sup>9</sup> The Li(1)–N(1) bond is longer than observed in the complexes  $[\text{Li}\{\text{N}(\text{Py})(\text{Ph})\}_2\{\text{HN}(\text{Py})(\text{Ph})\}(\text{HMPA})]$ <sup>10</sup> and  $[\{\text{Li}[\text{N}(\text{Py})(\text{Ph})](\text{HMPA})\}_2]$ ,<sup>11</sup> reflecting the larger coordination number of lithium in **2**. The trimethylsilyl group is staggered

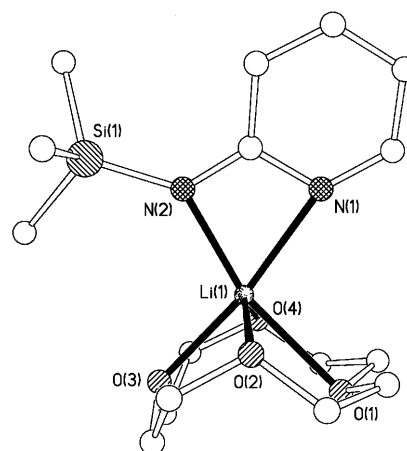


Fig. 1 Structure of **2** with selected atom labels; hydrogen atoms omitted for clarity.

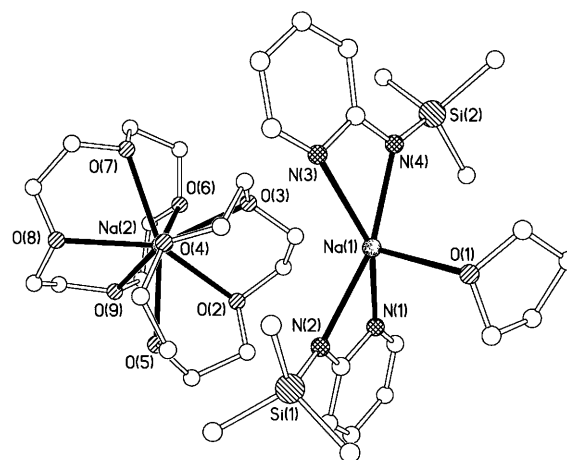


Fig. 2 Structure of **3** with selected atom labels; hydrogen atoms and disordered THF solvent omitted for clarity.

with respect to the pyridyl ring, presumably to minimise steric interactions. The 12-crown-4 is in a puckered conformation instead of the conformation observed in the complex  $[\text{LiNCS}(12\text{C}4)]$ .<sup>12</sup> The Li–O bond lengths are in the range 2.063(2)–2.284(2) Å, which is in agreement with the ranges reported for the complexes  $[\text{LiSCPh}_3(12\text{C}4)]$ <sup>13</sup> and  $[\text{Li}(2\text{-SC}_5\text{H}_4\text{N})(12\text{C}4)]$ .<sup>14</sup> This results in the lithium atom residing 1.128 Å above the mean plane of the crown oxygen atoms, which is an average between the two lower and higher oxygen pair positions. The amide coordinates to the lithium cation with a dihedral angle of 14.8° between the pyridyl ring and the N(1)–Li(1)–N(2) plane.

The molecular structure of **3** is illustrated in Fig. 2 and selected bond lengths can be found in Table 1. The complex crystallises as a solvent-separated ion pair ‘ate’ complex. A second molecule of THF co-crystallises uncoordinated in the structure and is disordered over two sites. The cation is a sodium centre sandwiched between two 12-crown-4 molecules in a staggered conformation exhibiting pseudo- $D_{4d}$  symmetry. The Na–O bond lengths span the range 2.4281(13)–2.5430(13) Å, in agreement with previously reported examples.<sup>14–17</sup> This results in the sodium cation residing 1.476 Å out of the mean oxygen plane of each crown. In all other respects the sandwich is essentially the same as other reported examples. Of particular interest is the ‘ate’ fragment. ‘Ate’ complexes are generally uncommon, and usually occur when solvation of one cation is strongly favoured, leaving the remaining cation to coordinate to both anions. Here the driving force is the solvation of one sodium cation by two 12-crown-4 molecules, resulting in two amide ligands coordinating to the other sodium cation in a *trans* manner. However, this does not satisfy the coordination

**Table 1** Selected bond lengths (Å) and angles (°)

<b>Compound 2</b>			
Li(1)–N(1)	2.203(2)	Li(1)–N(2)	2.057(2)
Li(1)–O(1)	2.284(2)	Li(1)–O(2)	2.170(2)
Li(1)–O(3)	2.063(2)	Li(4)–O(4)	2.210(2)
N(1)–Li(1)–N(2)	64.96(7)	O(1)–Li(1)–O(3)	89.26(8)
O(2)–Li(1)–O(4)	142.36(10)		
<b>Compound 3</b>			
Na(1)–N(1)	2.5352(13)	Na(1)–N(2)	2.3987(13)
Na(1)–N(3)	2.4606(13)	Na(1)–N(4)	2.4099(13)
Na(1)–O(1)	2.4170(14)		
Na(2)–O(2)	2.4641(13)	Na(2)–O(3)	2.4583(13)
Na(2)–O(4)	2.4281(13)	Na(2)–O(5)	2.5430(13)
Na(2)–O(6)	2.4553(13)	Na(2)–O(7)	2.4871(13)
Na(2)–O(8)	2.4943(13)	Na(2)–O(9)	2.4437(12)
N(1)–Na(1)–N(2)	55.42(4)	N(3)–Na(1)–N(4)	56.45(4)
<b>Compound 4</b>			
K(1)–N(1)	2.853(2)	K(1)–N(1A)	2.858(2)
K(1)–N(2)	2.858(2)	K(1)–N(2A)	2.912(2)
K(1)–O(1)	3.227(3)	K(1)–O(2)	2.778(2)
K(1)–O(3)	2.800(2)	K(1)–O(4)	2.816(2)
N(1)–K(1)–N(2)	47.60(5)	K(1)–N(1)–K(1A)	72.52(5)
K(1)–N(2)–K(1A)	71.66(5)		
<b>Compound 5</b>			
Rb(1)–N(1)	3.051(4)	Rb(1)–N(1A)	3.152(4)
Rb(1)–N(2)	2.990(4)	Rb(1)–N(2A)	2.922(4)
Rb(1)–O(1)	3.086(8)	Rb(1)–O(2)	3.774(7)
Rb(1)–O(3)	3.065(8)	Rb(1)–O(4)	2.832(5)
N(1)–Rb(1)–N(2)	44.94(10)	Rb(1)–N(1)–Rb(1A)	71.79(8)
Rb(1)–N(2)–Rb(1A)	75.94(9)		
<b>Compound 6</b>			
Cs(1)–N(1)	3.379(3)	Cs(1)–N(1A)	3.345(3)
Cs(1)–N(2)	3.194(4)	Cs(1)–N(2A)	3.216(4)
Cs(1)–O(5)	3.110(3)	Cs(1)–O(6)	3.362(3)
Cs(1)–O(7)	3.228(3)	Cs(1)–O(8)	3.098(3)
Cs(1)–O(4A)	3.258(3)	Cs(2)–N(2A)	3.367(4)
Cs(2)–N(3)	3.246(4)	Cs(2)–N(4B)	3.191(4)
Cs(2)–O(1)	3.227(3)	Cs(2)–O(2)	3.064(3)
Cs(2)–O(3)	3.256(3)	Cs(2)–O(4)	3.247(3)
Cs(2)–O(8)	3.200(3)		
N(1)–Cs(1)–N(2)	41.06(9)	N(1A)–Cs(1)–N(2A)	41.20(9)
Cs(1)–N(1)–Cs(1A)	75.94(7)	Cs(1)–N(2)–Cs(1A)	80.37(9)
Cs(1A)–O(4)–Cs(2)	89.48(6)	Cs(1)–O(8)–Cs(2)	89.94(8)
<b>Compound 7</b>			
Cs(1)–N(1)	3.252(5)	Cs(1)–N(1A)	3.255(5)
Cs(1)–N(2)	3.196(6)	Cs(1)–N(2A)	3.092(5)
Cs(1)–O(1)	3.211(5)	Cs(1)–O(2)	3.097(4)
Cs(1)–O(3)	3.264(5)	Cs(1)–O(4)	3.524(14)
N(1)–Cs(1)–N(2)	41.99(12)	Cs(1)–N(1)–Cs(1A)	76.49(10)
Cs(1)–N(2)–Cs(1A)	79.67(13)		

requirements of sodium, and a molecule of THF completes the coordination sphere. This contrasts with **2**, where the coordination sphere of the small lithium is filled by the crown and amide. Although solvation of lithium to form a sandwich is even more favourable, the resulting ‘ate’ fragment would be too sterically strained. The ‘ate’ sodium Na(1) is perhaps best described as having distorted square pyramidal coordination. This five-coordinate sodium is chiral, but the crystal structure is centrosymmetric, and therefore both enantiomers are present in equal amounts in the solid state. As for **2**, both trimethylsilyl groups are staggered with respect to the pyridyl rings. Turning to bond lengths, the sodium Na(1)–O(1) bond length of 2.4170(14) Å is substantially longer than the Na–O bond length of 2.385(8) Å reported in the closely related

‘ate’ fragment [Na(2-S-Py)<sub>2</sub>(THF)] in the solvent-separated ion quadruple [{Na(12C4)<sub>2</sub>}<sub>4</sub>{Na(2-S-Py)<sub>2</sub>(THF)}<sub>2</sub>{Na(2-S-Py)<sub>2</sub>}]<sub>2</sub>,<sup>14</sup> and is in the range reported for the complexes [LiN(SiMe<sub>3</sub>)<sub>2</sub>NaN(SiMe<sub>3</sub>)<sub>2</sub>(THF)<sub>3</sub>] and [NaN(SiMe<sub>3</sub>)<sub>2</sub>KN(SiMe<sub>3</sub>)<sub>2</sub>(THF)<sub>3</sub>].<sup>18</sup> The Na–N bond lengths consist of a short Na–amide pair of 2.3987(13) and 2.4099(13) Å and a long Na–pyridyl pair of 2.4606(13) and 2.5352(13) Å. These are shorter and longer respectively than those reported in the complexes [{Na[N(Py)(Ph)]<sub>2</sub>(HMPA)<sub>3</sub>}]<sup>19</sup> and [{NaN(Py)(Me)(TMEDA)}<sub>2</sub>]<sup>20</sup> reflecting the charge stabilising nature of the trimethylsilyl group. This gives natural bite angles of 55.42(4) and 56.45(4)°, which are substantially smaller angles than in **2**, reflecting the larger ionic radius of sodium compared to lithium. The reason for the large disparity of bond lengths

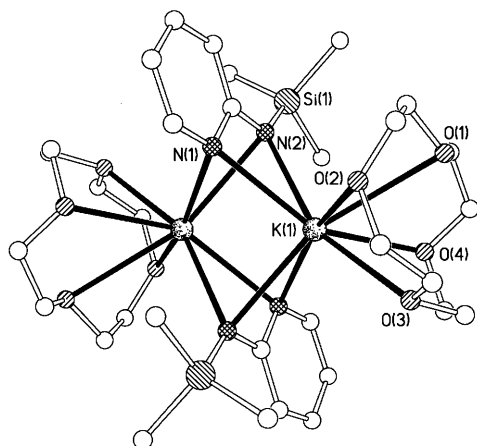


**Fig. 3** Structure of **4** with selected atom labels; hydrogen atoms and toluene solvent omitted for clarity. The structures of **5** and of **7** are very similar in general appearance.

between pairs is not clear, as there is very little difference in bond lengths within the two ligands.

The structure of **4** is shown in Fig. 3 and selected bond lengths can be found in Table 1. The complex crystallises as a discrete amide-bridged dimer based around a *transoid* (KN)<sub>2</sub> ring, with additional coordination of pyridyl groups, and capped on each end by a molecule of 12-crown-4. One molecule of toluene per molecule of **4** crystallises in the structure and is unremarkable. The molecule of **4** is exactly centrosymmetric, the (KN)<sub>2</sub> ring residing on a crystallographic inversion centre. This contrasts with **3** and indicates the preference of softer metal centres for formation of contact ion pairs compared to solvent-separated ion pairs. The 12-crown-4 molecules are distorted considerably, due to the close proximity of the bulky trimethylsilyl groups. The K–O bond lengths span the range 2.778(2)–3.227(3) Å due to the distortion of the crown coordination, resulting in one very long K–O bond. The other three K–O bond lengths compare well with those reported for the alkali complexes [K(18C6)(12C4)Na] and [K(18C6)(12C4)K].<sup>21</sup> This results in the potassium being displaced 2.535 Å from the mean oxygen plane of the crown. Turning to the amide, the K–N bond lengths span the ranges 2.858(2)–2.912(2) Å (amide) and 2.853(2)–2.858(2) Å (pyridyl). There is essentially a reversal in the expected trend of bond lengths. With the charge stabilising nature of the trimethylsilyl group the K–amide bonds would be expected to be short with longer K–pyridyl bonds. This may be a result of the large bulk of the trimethylsilyl groups, preventing closer approach of the amide centres to the metals. Nevertheless, the observed K–amide bond lengths are in good agreement with those reported in the antimony(III) complex [K{(Cy)N(H)Sb(μ-NCy)<sub>2</sub>}]<sub>2</sub>·2(THF) (Cy = cyclohexyl)<sup>22</sup> and the K–pyridyl bond lengths are comparable to those reported in the closely related complex [K{N(Py)(Ph)}(TMEDA)]<sub>2</sub>.<sup>20</sup> The trimethylsilyl groups are again staggered with respect to the pyridyl rings, presumably to minimise steric interaction. The pyridyl rings are tilted away from being normal to the K(1)–K(2) vector. The N(1) pyridyl ring tilts away from K(1).

Selected bond lengths for **5** are in Table 1. The complex crystallises as a contact ion pair dimer of the same general architecture as **4**, based around a *transoid* (RbN)<sub>2</sub> ring with additional coordination of pyridyl groups, and capped on each end by a molecule of 12-crown-4. The molecule is centrosymmetric, the (RbN)<sub>2</sub> ring residing on a crystallographic inversion centre. The 12-crown-4 molecules are distorted considerably, presumably due to the close proximity of the bulky trimethylsilyl groups and the poor host–guest fit with rubidium. This results in three Rb–O bond lengths that span the range 2.832(5)–3.086(8) Å, with an appreciably longer Rb–O(2) bond

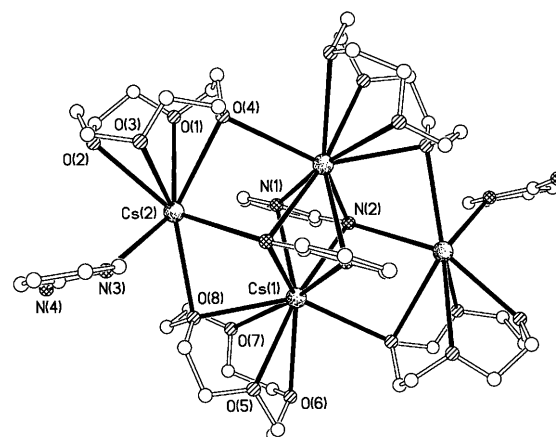


**Fig. 4** Structure of the tetranuclear unit of **6** with selected atom labels; hydrogen atoms omitted for clarity.

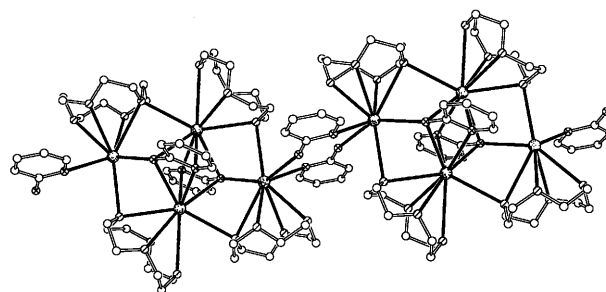


**Fig. 5** Two units of the polymeric structure of **6**; hydrogen atoms omitted for clarity.

length of 3.774(7) Å. Rubidium is displaced 2.303 Å from the mean oxygen plane of the crown. For the amide, the Rb–N bond lengths span the ranges 2.922(4)–2.990(4) Å (amide) and 3.051(4)–3.152(4) Å (pyridyl). These are higher values than in **4**, reflecting the larger ionic radius of rubidium compared to potassium. With the charge stabilising nature of the trimethylsilyl group the amide bonds would be expected to be short with longer pyridyl bonds, and indeed this is the case, unlike in **4**, reflecting the larger size of rubidium. The Rb–pyridyl bond lengths are at the higher end of the range associated with tertiary amines bonded to rubidium. For example, bond lengths in the ranges 3.022–3.099 and 3.092–3.131 Å have been reported in the complexes [Rb(fluorenyl)(PMDETA)]<sub>2</sub><sup>23</sup> and [RbC(H)(SiMe<sub>3</sub>)<sub>2</sub>(PMDETA)]<sub>2</sub><sup>24</sup> (PMDETA = *N,N,N',N',N'*-pentamethyldiethylenetriamine). The Rb–amide bond lengths fall within the range of values previously reported.<sup>25,26,27</sup> The trimethylsilyl groups are again staggered with respect to the pyridyl rings. The pyridyl rings are tilted away from being normal to the Rb(1)–Rb(1A) vector, slightly more (by about 4°) than in **4**, reflecting the increased preference of the larger, softer rubidium for incipient multi-hapto interaction with the π system of the pyridyl ring.

The basic unit of the structure of **6** is illustrated in Fig. 4 and selected bond lengths are in Table 1. The complex crystallises as an unprecedented tetranuclear cluster in the solid state. Other reported examples of homo-tetranuclear/tetrameric caesium clusters display cubane architectures.<sup>28,29</sup> The cluster consists of a bridged *trans* dimer core, of similar architecture to **4** and **5**, with additional caesium centres grafted on to each side of the core by bridging oxygens from the 12-crown-4 molecules. The cluster is linked by bridging pyridylamide ligands from the grafted caesium centres to corresponding ones in the next cluster to form an infinite polymer in the solid state, as is illustrated in Fig. 5. The cluster is centrosymmetric with one bridging and one grafted caesium (and associated crowns and amides) in the asymmetric unit. It is pertinent to note that the grafted caesium centres lie approximately where, had they been

present, the trimethylsilyl groups would have been. Clearly the amide hydrogens do not have the steric bulk to prevent further aggregation of the dimer core. Also, although two equivalents of 12-crown-4 were available, only one equivalent is present in the solid state structure, reflecting the unfavourable host–guest fit. The Cs–O bond lengths span the range 3.064(3)–3.362(3) Å. These are longer bonds than observed in **5**, in keeping with the larger ionic radius of caesium compared to rubidium. There is a steady decline in the number of known structures of complexes with 12-crown-4 complexed to the alkali metals as the group is descended, and this appears to be the first crystallographic example of a caesium complex coordinated by 12-crown-4. However, the range of Cs–O bond lengths is in good agreement with previously reported examples of Cs–O bond lengths with neutral donor ligands.<sup>26,27</sup> This results in the caesium centres residing 2.480 Å [Cs(1)] and 2.492 Å [Cs(2)] from the mean oxygen planes of the respective crowns, a larger deviation than with rubidium, reflecting the poorer host–guest fit. Dealing with the bridging core amides first, there are two short Cs–N amide bonds [3.194(4) and 3.216(4) Å] and two longer Cs–N pyridyl bonds [3.379(3) and 3.345(3) Å]. The Cs–amide bond lengths are at the higher range of previously reported Cs–N bond lengths, as expected for bridging centres. For example, a Cs–N bond length of 2.991 Å has been reported for the complex  $\{[Cs\{N(Ph)N(SiMe_3)_2\}]_2\}_n$ ,<sup>30</sup> and lengths of 3.071 Å and 3.045–3.249 Å have been reported in the bridged complexes  $[(Me_3Si)_2NCs_2Sn(CH_2Ph)\{Si(SiMe_3)_3\}_2]$ <sup>31</sup> and  $\{[Cs(Me_3SiN)_2S(Ph)](THF)\}_2$ .<sup>32</sup> The Cs–pyridyl bond lengths are in the range of previously reported complexes. For example, ranges of 3.160–3.326 and 3.175–3.639 Å have been reported for the complexes  $\{[CsC(Ph)_3(PMDETA)]_2\}_n$ <sup>33</sup> and  $\{[Cs(TMEDA)-C_4B_8H_8(SiMe_3)_4Cs]\}_n$ .<sup>34</sup> The trend of increasing ring tilt and increased tendency to multihapto interaction observed with the potassium and rubidium dimers, is extended with this complex, with a further increase of about 6°. N(2) also has a fifth contact of 3.367(4) Å to the grafted Cs(2) centre. This apparent five-coordinate ligand atom is not unusual in alkali metal chemistry, where five-coordinate ‘carbanion’ alkyl centres are frequently observed.<sup>35</sup> The Cs(2) centre bridges to another cluster *via* two bridging amides with a short amide bond of 3.191(4) and a longer pyridyl bond of 3.246(4) Å. These are both correspondingly shorter than in the central core, as would be expected for terminal Cs–N bonds.

Selected bond lengths and angles for **7** can be found in Table 1. The complex, similar in general appearance to **4** and **5**, crystallises as a contact ion pair dimer with no significant intermolecular interactions. A highly disordered molecule of toluene crystallises in the structure. The dimer consists of the now familiar bridged dimer core architecture of a (CsN)<sub>2</sub> ring with additional coordination by the pyridyl nitrogens. The (CsN)<sub>2</sub> ring is *trans* as a result of residing over a crystallographic inversion centre. The coordination sphere of each caesium is completed by a molecule of 12-crown-4 capping each end of the dimer. The Cs–O bond lengths span the range 3.097(4)–3.524(14), which is a larger range than in **6**, but in good agreement when the longest bond is discounted. This long bond is presumably due to the poor host–guest fit and the presence of the bulky trimethylsilyl group. This results in the caesium being displaced 2.605 Å from the mean oxygen plane of the crown, reflecting the presence of the longer bond. The Cs–N bond lengths span the ranges 3.092(5)–3.196(6) Å (amide) and 3.252(5)–3.255(5) Å (pyridyl). These are both slightly shorter values than in **6**, reflecting the less sterically encumbered environment around the caesium centres. However, they do fit within the range of values described earlier. Interestingly, the pyridyl ring tilt in this dimer is almost identical to that in **6**. This results in almost identical dimer cores of **6** and **7**. The trimethylsilyl group is again staggered with respect to the pyridyl ring and it can be clearly seen that a methyl group is occupying the space that the grafted caesium occupies in **6**. This

is a clear example of how a peripheral modification can drastically alter the molecular and crystal structure adopted by a complex.

## Conclusions

The secondary amine 2-trimethylsilylaminopyridine is readily accessible *via* a simple synthetic procedure and undergoes facile deprotonation with Bu<sup>n</sup>Li to give the corresponding lithium amide. Heavier alkali metal derivatives of this ligand are, with the exception of caesium, readily prepared by metathesis with the appropriate heavier alkali metal alkoxides. Room temperature metathesis with caesium 2-ethylhexoxide generates a primary amide caesium complex with concomitant cleavage of the N–Si bond. Synthesis of the silylated caesium complex is accomplished by low temperature synthesis. Structural studies show a dominance of contact ion pairs based upon the (MN)<sub>2</sub> ring prevalent in alkali metal amide chemistry. A distinct tendency towards multihapto interactions with the π systems of the pyridyl rings is apparent with the heavier alkali metals. In contrast, the unusual sodium ‘ate’ complex is formed by the favourable solvation of a sodium cation. Studies of alkali metal complexes of **1**, and related amides, with other crown ethers are currently under investigation.

## Experimental

### General

All manipulations were carried out using standard Schlenk techniques under an atmosphere of dry nitrogen. Methylcyclohexane, benzene, toluene, diethyl ether and THF were distilled from sodium–benzophenone ketyl under an atmosphere of dry nitrogen and stored over activated 4A molecular sieves. HMPA was dried over CaH<sub>2</sub> and stored over activated 4 A molecular sieves. 12-Crown-4 was dried by, and stored over, activated 4 A molecular sieves. Deuterated solvents were distilled from a potassium mirror, deoxygenated by three freeze–pump–thaw cycles and stored over activated 4 A molecular sieves. Chlorotrimethylsilane, 2-aminopyridine, Bu<sup>n</sup>ONa and Bu<sup>n</sup>OK were used without further purification. Butyllithium was purchased from Aldrich as a 2.5 M solution in hexanes. Rubidium 2-ethylhexoxide and caesium 2-ethylhexoxide were prepared by a literature method.<sup>28</sup>

The <sup>1</sup>H and <sup>13</sup>C NMR spectra were recorded on a Bruker AC200 spectrometer and <sup>7</sup>Li, <sup>29</sup>Si and <sup>133</sup>Cs spectra on a Bruker WM300 spectrometer operating at 200.1, 50.3, 116.6, 59.6 and 39.4 MHz respectively; <sup>1</sup>H, <sup>13</sup>C and <sup>29</sup>Si chemical shifts are quoted in ppm relative to tetramethylsilane, <sup>7</sup>Li chemical shifts relative to external 1.0 M LiCl and <sup>133</sup>Cs chemical shifts relative to external 0.01 M CsI. Elemental analyses were carried out by Elemental Microanalysis Ltd., Okehampton, UK.

### Preparations

**[PyN(H)SiMe<sub>3</sub>] 1.** A 100 mL Schlenk flask was charged with 2-aminopyridine (2.90 g, 30.80 mmol) dissolved in diethyl ether (80 mL). The solution was cooled to 0 °C and Bu<sup>n</sup>Li (12.32 mL, 30.8 mmol) added dropwise, and the solution stirred for 1.5 h and allowed to warm to room temperature. The solution was cooled to 0 °C and Me<sub>3</sub>SiCl (5.0 mL, 39.0 mmol) was added dropwise; stirring continued overnight to give a white precipitate. The solution was filtered from the precipitate and volatiles were removed *in vacuo* to give a yellow oil. Distillation at 1 mm Hg/35 °C gave **1** as a viscous colourless oil (4.88 g, 95.3%). Spectroscopic data for **1**: δ<sub>H</sub> ([<sup>2</sup>H]<sub>8</sub>-THF) 0.43 (9H, s, SiMe<sub>3</sub>), 3.96 (1H, s, br, N–H), 6.20 (1H, d, β'-H of Py), 6.48 (1H, t, β-H of Py), 7.17 (1H, t, γ-H of Py) and 8.27 (1H, d, α-H of Py). δ<sub>C</sub> ([<sup>2</sup>H]<sub>8</sub>-THF) 0.23 (SiMe<sub>3</sub>), 109.89 (β'-C of Py), 113.01 (β-C of Py), 136.93 (γ-C of Py), 148.20 (α-C of Py) and 160.25 (α'-C of Py). δ<sub>Si</sub> ([<sup>2</sup>H]<sub>8</sub>-THF) 2.43 (s, SiMe<sub>3</sub>).

**[Li(PyNSiMe<sub>3</sub>)(12C4)] 2.** A 100 mL Schlenk flask was charged with 2-trimethylsilylaminopyridine (0.56 g, 3.36 mmol) and 12-crown-4 (0.56 mL, 3.36 mmol) dissolved in THF (40 mL). Dropwise addition of Bu<sup>n</sup>Li (1.35 mL, 3.36 mmol) afforded a yellow solution. Upon stirring overnight the solution turned red. Removal of volatiles *in vacuo* yielded a viscous deep red oil. Recrystallisation from a methylcyclohexane–THF solution at 5 °C gave crystals of **2** suitable for crystallographic study (1.0 g, 85.4%). Microanalysis for **2**: C, 54.97; H, 8.67; N, 7.88. C<sub>16</sub>H<sub>29</sub>N<sub>2</sub>O<sub>4</sub>SiLi requires C, 55.15; H, 8.39; N, 8.04%. Spectroscopic data:  $\delta_{\text{H}}$  ([<sup>2</sup>H]<sub>8</sub>-THF) 0.12 (9H, s, SiMe<sub>3</sub>), 3.69 (16H, s, 12C4), 5.91 (1H, t,  $\beta$ -H of Py), 6.19 (1H, d,  $\beta'$ -H of Py), 6.98 (1H, t,  $\gamma$ -H of Py) and 7.64 (1H, d,  $\alpha$ -H of Py).  $\delta_{\text{C}}$  ([<sup>2</sup>H]<sub>8</sub>-THF) 3.36 (SiMe<sub>3</sub>), 72.52 (12C4), 106.43 ( $\beta$ -C of Py), 115.35 ( $\beta'$ -C of Py), 137.60 ( $\gamma$ -C of Py), 148.99 ( $\alpha$ -C of Py) and 172.85 ( $\alpha'$ -C of Py).  $\delta_{\text{Li}}$  ([<sup>2</sup>H]<sub>8</sub>-THF) 1.17 (s).  $\delta_{\text{Si}}$  ([<sup>2</sup>H]<sub>8</sub>-THF) –13.38 (s, SiMe<sub>3</sub>).

**[Na(12C4)<sub>2</sub>][Na(PyNSiMe<sub>3</sub>)<sub>2</sub>(THF)]·(THF) 3.** A 100 mL Schlenk flask was charged with 2-trimethylsilylaminopyridine (0.43 g, 2.59 mmol) and 12-crown-4 (0.42 mL, 2.59 mmol) dissolved in THF (40 mL). Dropwise addition of Bu<sup>n</sup>Li (1.04 mL, 2.59 mmol) afforded a yellow solution. Addition of this solution to Bu<sup>n</sup>ONa (0.25 g, 2.59 mmol) gave a deep red solution. Removal of volatiles *in vacuo* yielded a viscous deep red oil. Recrystallisation from THF at –30 °C gave crystals of **3** suitable for crystallography (0.94 g, 83.2%). Microanalysis for **3**: C, 53.01; H, 8.62; N, 6.39. C<sub>36</sub>H<sub>66</sub>N<sub>4</sub>O<sub>9</sub>Si<sub>2</sub>Na<sub>2</sub>·C<sub>4</sub>H<sub>8</sub>O requires C, 55.02; H, 8.54; N, 6.42%. Spectroscopic data:  $\delta_{\text{H}}$  ([<sup>2</sup>H]<sub>8</sub>-THF) 0.10 (18H, s, SiMe<sub>3</sub>), 1.85 (4H, m, CH<sub>2</sub> of THF), 3.64 (32H, s, 12C4), 3.67 (4H, m, OCH<sub>2</sub> of THF), 5.72 (2H, t,  $\beta$ -H of Py), 6.06 (2H, d,  $\beta'$ -H of Py), 6.83 (2H, t,  $\gamma$ -H of Py) and 7.70 (2H, d,  $\alpha$ -H of Py).  $\delta_{\text{C}}$  ([<sup>2</sup>H]<sub>8</sub>-THF) 2.56 (SiMe<sub>3</sub>), 25.2 (CH<sub>2</sub> of THF), 67.31 (OCH<sub>2</sub> of THF), 67.72 (12C4), 103.45 ( $\beta$ -C of Py), 114.42 ( $\beta'$ -C of Py), 135.09 ( $\gamma$ -C of Py), 149.34 ( $\alpha$ -C of Py) and 170.55 ( $\alpha'$ -C of Py).  $\delta_{\text{Si}}$  ([<sup>2</sup>H]<sub>8</sub> THF) –17.40 (s, SiMe<sub>3</sub>).

**[{K(PyNSiMe<sub>3</sub>)(12C4)<sub>2</sub>}]<sub>2</sub>·2PhMe 4.** A 100 mL Schlenk flask was charged with 2-trimethylsilylaminopyridine (0.52 g, 3.13 mmol) and 12-crown-4 (0.50 mL, 3.13 mmol) dissolved in THF (40 mL). Dropwise addition of Bu<sup>n</sup>Li (1.25 mL, 3.13 mmol) afforded a yellow solution. Addition of this solution to Bu<sup>n</sup>OK (0.35 g, 3.13 mmol) gave a deep orange solution. Removal of volatiles *in vacuo* yielded a viscous deep red oil. Recrystallisation from toluene solution at 5 °C gave crystals of **4** suitable for crystallography (0.78 g, 58.4%). Microanalysis for **4**: C, 50.03; H, 7.36; N, 6.69. C<sub>32</sub>H<sub>58</sub>N<sub>4</sub>O<sub>8</sub>Si<sub>2</sub>K<sub>2</sub> requires C, 50.49; H, 7.68; N, 7.36%. Spectroscopic data:  $\delta_{\text{H}}$  ([<sup>2</sup>H]<sub>8</sub>-THF) 0.14 (18H, s, SiMe<sub>3</sub>), 3.60 (32H, s, 12C4), 5.81 (2H, t,  $\beta$ -H of Py), 6.12 (2H, d,  $\beta'$ -H of Py), 6.86 (2H, t,  $\gamma$ -H of Py) and 7.77 (2H, d,  $\alpha$ -H of Py).  $\delta_{\text{C}}$  ([<sup>2</sup>H]<sub>8</sub>-THF) 2.49 (SiMe<sub>3</sub>), 69.36 (12C4), 103.79 ( $\beta$ -C of Py), 115.28 ( $\beta'$ -C of Py), 135.21 ( $\gamma$ -C of Py), 149.67 ( $\alpha$ -C of Py) and 170.09 ( $\alpha'$ -C of Py).  $\delta_{\text{Si}}$  ([<sup>2</sup>H]<sub>8</sub>-THF) –17.39 (s, SiMe<sub>3</sub>).

**[{Rb(PyNSiMe<sub>3</sub>)(12C4)<sub>2</sub>}] 5.** A 100 mL Schlenk flask was charged with 2-trimethylsilylaminopyridine (0.57 g, 3.43 mmol) and 12-crown-4 (0.55 mL, 3.43 mmol) dissolved in THF (40 mL). Dropwise addition of Bu<sup>n</sup>Li (1.37 mL, 3.43 mmol) afforded a yellow solution. Addition of this solution to rubidium 2-ethylhexoxide (0.74 g, 3.43 mmol) gave a cloudy dark orange solution. Filtration and removal of volatiles *in vacuo* yielded a viscous deep red oil. Recrystallisation from toluene solution at 5 °C gave crystals of **5** suitable for crystallography (0.88 g, 60.2%). Microanalysis for **5**: C, 44.88; H, 7.09; N, 6.31. C<sub>32</sub>H<sub>58</sub>N<sub>4</sub>O<sub>8</sub>Si<sub>2</sub>Rb<sub>2</sub> requires C, 45.01; H, 6.85; N, 6.56%. Spectroscopic data:  $\delta_{\text{H}}$  ([<sup>2</sup>H]<sub>8</sub>-THF) 0.12 (18H, s, SiMe<sub>3</sub>), 3.58 (32H, s, 12C4), 5.78 (2H, t,  $\beta$ -H of Py), 6.11 (2H, d,  $\beta'$ -H of Py), 6.85 (2H, t,  $\gamma$ -H of Py) and 7.76 (2H, d,  $\alpha$ -H of Py).  $\delta_{\text{C}}$  ([<sup>2</sup>H]<sub>8</sub>-THF) 2.60 (SiMe<sub>3</sub>), 70.01 (12C4), 104.01 ( $\beta$ -C of Py), 115.86 ( $\beta'$ -C of Py), 135.38 ( $\gamma$ -C of Py), 149.75 ( $\alpha$ -C of Py) and 169.85 ( $\alpha'$ -C of Py).  $\delta_{\text{Si}}$  ([<sup>2</sup>H]<sub>8</sub>-THF) –17.87 (s, SiMe<sub>3</sub>).

**[{Cs(PyNH)(12C4)<sub>2</sub>}] 6.** A 100 mL Schlenk flask was charged with 2-trimethylsilylaminopyridine (0.63 g, 3.79 mmol) and 12-crown-4 (1.22 mL, 7.58 mmol) dissolved in THF (40 mL). Dropwise addition of Bu<sup>n</sup>Li (1.52 mL, 3.79 mmol) afforded a yellow solution. Addition of this solution to caesium 2-ethylhexoxide (0.99 g, 3.79 mmol) gave a cloudy deep orange solution. Filtration and removal of volatiles *in vacuo* yielded a viscous deep red oil. Recrystallisation from a methylcyclohexane–HMPA solution at 5 °C gave crystals of **6** suitable for X-ray diffraction (0.92 g, 60.4%). Microanalysis for **6**: C, 38.83; H, 5.37; N, 6.91. C<sub>52</sub>H<sub>84</sub>N<sub>8</sub>O<sub>16</sub>Cs<sub>4</sub> requires C, 38.83; H, 5.26; N, 6.96%. Spectroscopic data:  $\delta_{\text{H}}$  ([<sup>2</sup>H]<sub>8</sub>-THF) 3.73 (64H, s, 12C4), 3.79 (4H, s, N–H), 5.93 (4H, t,  $\beta$ -H of Py), 6.23 (4H, d,  $\beta'$ -H of Py), 6.96 (4H, t,  $\gamma$ -H of Py) and 7.72 (4H, d,  $\alpha$ -H of Py).  $\delta_{\text{C}}$  ([<sup>2</sup>H]<sub>8</sub>-THF) 71.74 (12C4), 106.80 ( $\beta$ -C of Py), 112.92 ( $\beta'$ -C of Py), 135.82 ( $\gamma$ -C of Py), 149.23 ( $\alpha$ -C of Py) and 170.87 ( $\alpha'$ -C of Py).  $\delta_{\text{Cs}}$  ([<sup>2</sup>H]<sub>8</sub> THF) 29.84 (s, br).

**[{Cs(PyNSiMe<sub>3</sub>)(12C4)<sub>2</sub>}]<sub>2</sub>·PhMe 7.** A 100 mL Schlenk flask was charged with 2-trimethylsilylaminopyridine (0.42 g, 2.53 mmol) and 12-crown-4 (0.41 mL, 2.53 mmol) dissolved in THF (40 mL). Dropwise addition of Bu<sup>n</sup>Li (1.01 mL, 2.53 mmol) afforded a yellow solution. The solution was cooled to –78 °C. Dropwise addition of caesium 2-ethylhexoxide (0.66 g, 2.53 mmol) in methylcyclohexane (3.2 mL) gave a yellow precipitate. The solution was allowed to warm slowly to room temperature resulting in dissolution of the precipitate to give an orange solution. Removal of volatiles *in vacuo* yielded a viscous deep red oil. Recrystallisation from toluene at 5 °C gave crystals of **7** suitable for X-ray crystallography (0.86 g, 71.6%). Microanalysis for **7**: C, 38.48; H, 6.64; N, 5.98. C<sub>32</sub>H<sub>58</sub>N<sub>4</sub>O<sub>8</sub>Si<sub>2</sub>Cs<sub>2</sub> requires C, 40.51; H, 6.16; N, 5.90%. Spectroscopic data:  $\delta_{\text{H}}$  ([<sup>2</sup>H]<sub>8</sub>-THF) 0.13 (18H, s, SiMe<sub>3</sub>), 3.61 (32H, s, 12C4), 5.77 (2H, t,  $\beta$ -H of Py), 5.80 (2H, d,  $\beta'$ -H of Py), 6.86 (2H, t,  $\gamma$ -H of Py) and 7.79 (2H, d,  $\alpha$ -H of Py).  $\delta_{\text{C}}$  ([<sup>2</sup>H]<sub>8</sub>-THF) 2.57 (SiMe<sub>3</sub>), 71.00 (12C4), 104.10 ( $\beta$ -C of Py), 116.63 ( $\beta$ -C of Py), 135.38 ( $\gamma$ -C of Py), 149.54 ( $\alpha$ -C of Py) and 169.11 ( $\alpha'$ -C of Py).  $\delta_{\text{Si}}$  ([<sup>2</sup>H]<sub>8</sub>-THF) –18.22 (s, SiMe<sub>3</sub>).  $\delta_{\text{Cs}}$  ([<sup>2</sup>H]<sub>8</sub> THF) 51.40 (s).

### X-Ray crystallography

Crystal data for complexes **2–7** are listed in Table 2. Crystals were examined on a Bruker AXS SMART CCD area detector diffractometer with graphite-monochromated Mo-K $\alpha$  radiation ( $\lambda = 0.71073$  Å), but with synchrotron radiation ( $\lambda = 0.6930$  Å)<sup>36</sup> for **7**. Cell parameters were refined from positions of all strong reflections in each data set. Intensities were corrected semi-empirically for absorption, based on symmetry-equivalent and repeated reflections. The structures were solved by direct methods or Patterson synthesis and refined on  $F^2$  values for all unique data. All non-hydrogen atoms were refined anisotropically. All hydrogen atoms, except amide N–H, were constrained with a riding model;  $U(\text{H})$  was set at 1.2 (1.5 for methyl groups) times  $U_{\text{eq}}$  for the parent atom. Disorder of the uncoordinated THF solvent in **3** was resolved over two sites with essentially equal contributions. Possible unresolved disorder in 12-crown-4 ligands is indicated by highly anisotropic displacements for some atoms in **4** and **5** and by some residual electron density features in **4** and **7**; otherwise the largest features are close to Cs atoms in **6** and **7**. Toluene solvent in **7** was too highly disordered for individual atoms to be resolved; this was treated by the SQUEEZE procedure of PLATON,<sup>37</sup> which indicated the correct total electron density and void volume for one molecule of toluene per dimer of the complex. Other programs were Bruker AXS SMART (control) and SAINT integration,<sup>38</sup> and SHELXTL for structure solution, refinement, and molecular graphics.<sup>39</sup>

CCDC reference numbers 152062–152067.

See <http://www.rsc.org/suppdata/dt/b0/b008852h/> for crystallographic data in CIF or other electronic format.

**Table 2** Crystallographic data for compounds 2–7

Compound	2	3	4	5	6	7
Formula	C <sub>16</sub> H <sub>29</sub> LiN <sub>2</sub> O <sub>4</sub> Si	[C <sub>16</sub> H <sub>32</sub> O <sub>8</sub> Na] <sup>+</sup> [C <sub>20</sub> H <sub>34</sub> N <sub>4</sub> NaOSi <sub>2</sub> ] <sup>-</sup> C <sub>4</sub> H <sub>8</sub> O	C <sub>32</sub> H <sub>58</sub> K <sub>2</sub> N <sub>4</sub> O <sub>8</sub> Si <sub>2</sub> · 2C <sub>7</sub> H <sub>8</sub>	C <sub>32</sub> H <sub>58</sub> N <sub>4</sub> O <sub>8</sub> Rb <sub>2</sub> Si <sub>2</sub>	C <sub>52</sub> H <sub>84</sub> Cs <sub>4</sub> N <sub>8</sub> O <sub>16</sub>	C <sub>32</sub> H <sub>58</sub> Cs <sub>2</sub> N <sub>4</sub> O <sub>8</sub> Si <sub>2</sub> · C <sub>7</sub> H <sub>8</sub>
Formula weight	348.4	873.2	945.5	853.9	1608.9	1041.0
Crystal system	Monoclinic	Monoclinic	Triclinic	Triclinic	Triclinic	Triclinic
Space group	<i>P</i> 2 <sub>1</sub> / <i>n</i>	<i>P</i> 2 <sub>1</sub> / <i>n</i>	<i>P</i> $\bar{1}$	<i>P</i> $\bar{1}$	<i>P</i> $\bar{1}$	<i>P</i> $\bar{1}$
<i>a</i> /Å	9.9095(3)	13.3161(5)	10.5289(7)	9.8861(15)	10.7464(7)	10.4715(12)
<i>b</i> /Å	12.2197(4)	22.3535(8)	11.6308(8)	10.0654(15)	11.5129(7)	10.9862(13)
<i>c</i> /Å	16.2582(5)	17.0658(6)	11.9792(8)	11.9755(17)	13.7340(8)	12.0328(14)
$\alpha$ /°			71.065(2)	106.949(2)	93.177(2)	65.913(2)
$\beta$ /°	99.935(2)	106.458(2)	88.749(2)	108.155(2)	111.692(2)	71.886(2)
$\gamma$ /°			72.796(2)	91.402(2)	93.177(2)	83.028(2)
<i>U</i> /Å <sup>3</sup>	1939.20(11)	4871.7(3)	1321.03(15)	1074.4(3)	1571.16(17)	1201.1(2)
<i>Z</i>	4	4	1	1	1	1
Data collected, unique	13559, 3421	33676, 8555	11488, 6034	7660, 3719	15504, 8156	9763, 5365
<i>R</i> <sub>int</sub>	0.0137	0.0196	0.0323	0.0392	0.0319	0.0444
Parameters	221	576	285	220	367	221
<i>R</i> , <i>R</i> <sub>w</sub> <sup>a</sup>	0.0277, 0.0749	0.0336, 0.0962	0.0564, 0.1547	0.0534, 0.1318	0.0371, 0.0871	0.0550, 0.1347
Diff. map extremes/e Å <sup>-3</sup>	+0.28, -0.24	+0.39, -0.27	+1.12, -0.48	+0.82, -0.80	+2.04, -2.14	+1.50, -1.66

<sup>a</sup> *R* on *F* values for data with  $F^2 > 2\sigma$ ; *R*<sub>w</sub> on all unique  $F^2$  values.

## Acknowledgements

We wish to thank EPSRC for equipment funding (W. C.) and the University of Newcastle upon Tyne for a studentship (S. T. L.).

## References

- W. N. Setzer and P. von R. Schleyer, *Adv. Organomet. Chem.*, 1985, **24**, 353.
- C. Schade and P. von R. Schleyer, *Adv. Organomet. Chem.*, 1987, **27**, 169.
- K. Gregory, P. von R. Schleyer and R. Snaith, *Adv. Inorg. Chem.*, 1991, **37**, 47.
- R. E. Mulvey, *Chem. Soc. Rev.*, 1991, **20**, 167.
- M. A. Beswick and D. S. Wright, in *Comprehensive Organometallic Chemistry II*, Eds. E. W. Abel, F. G. A. Stone and G. Wilkinson, Pergamon Press, Oxford, 1995, 1.
- J. D. Smith, *Adv. Organomet. Chem.*, 1999, **43**, 267.
- R. Snaith, in *Specialist Periodical Reports, Organometallic Chemistry*, vol. 26, The Royal Society of Chemistry, Cambridge, 1998, 1.
- L. M. Engelhardt, G. E. Jacobsen, P. C. Junk, C. L. Raston, B. W. Skelton and A. H. White, *J. Chem. Soc., Dalton Trans.*, 1988, 1011.
- H. Chen, R. A. Bartlett, H. V. R. Dias, M. M. Olmstead and P. P. Power, *J. Am. Chem. Soc.*, 1989, **111**, 4338.
- D. Barr, W. Clegg, R. E. Mulvey and R. Snaith, *J. Chem. Soc., Chem. Commun.*, 1984, 469.
- D. Barr, W. Clegg, R. E. Mulvey and R. Snaith, *J. Chem. Soc., Chem. Commun.*, 1984, 700.
- P. Groth, *Acta Chem. Scand., Ser. A*, 1981, **35**, 463.
- S. Chadwick, U. Englisch, M. O. Senge and K. Ruhlandt-Senge, *Inorg. Chem.*, 1996, **35**, 5820.
- S. Chadwick and K. Ruhlandt-Senge, *Chem. Eur. J.*, 1998, **4**, 1768.
- H. A. Eick and E. Mason, *Acta Crystallogr., Sect. B*, 1982, **38**, 1821.
- R. D. Rogers, L. K. Kurihara and M. M. Benning, *Inorg. Chem.*, 1987, **26**, 4346.
- M. Karl, G. Seybert, W. Massa, K. Harms, S. Agarwal, R. Maleika, W. Stelter, A. Greiner and W. Heitz, *Z. Anorg. Allg. Chem.*, 1999, **625**, 1301.
- P. G. Williard and M. A. Nichols, *J. Am. Chem. Soc.*, 1991, **113**, 9671.
- P. C. Andrews, W. Clegg and R. E. Mulvey, *Angew. Chem., Int. Ed. Engl.*, 1990, **29**, 1440.
- P. C. Andrews, D. R. Baker, W. Clegg, R. E. Mulvey and P. A. O'Neil, *Polyhedron*, 1991, **10**, 1839.
- R. H. Huang, J. L. Eglin, S. Z. Huang and L. E. H. McMills, J. L. Dye, *J. Am. Chem. Soc.*, 1993, **115**, 9542.
- A. Bashall, M. A. Beswick, C. N. Harmer, A. D. Hopkins, M. McPartlin, M. A. Paver, P. R. Raithby and D. S. Wright, *J. Chem. Soc., Dalton Trans.*, 1998, 1389.
- D. Hoffmann, F. Hampel and P. von R. Schleyer, *J. Organomet. Chem.*, 1993, **456**, 13.
- P. B. Hitchcock, M. F. Lappert, W. P. Leung, L. Diansheng and T. Shun, *J. Chem. Soc., Chem. Commun.*, 1993, 1386.
- A. Steiner and D. Stalke, *Inorg. Chem.*, 1993, **32**, 1977.
- T. Kottke and D. Stalke, *Organometallics*, 1996, **15**, 4552.
- F. T. Edelmann, F. Pauer, M. Wedler and D. Stalke, *Inorg. Chem.*, 1992, **31**, 4143.
- M. H. Chisholm, S. R. Drake, A. A. Naini and W. E. Streib, *Polyhedron*, 1991, **10**, 337.
- K. F. Tesh, B. D. Jones, T. P. Hanusa and J. C. Huffman, *Angew. Chem., Int. Ed. Engl.*, 1992, **114**, 6590.
- B. Gemünd, H. Nöth, H. Sachdev and M. Schmidt, *Chem. Ber.*, 1996, **129**, 1335.
- K. W. Klinkhammer, Thesis, University of Stuttgart, 1998.
- F. Pauer and D. Stalke, *J. Organomet. Chem.*, 1991, **418**, 127.
- D. Hoffmann, W. Bauer, P. von R. Schleyer, U. Pieper and D. Stalke, *Organometallics*, 1993, **12**, 1193.
- N. S. Hosmane, T. Demissie, H. Zhang, J. A. Maguire, W. N. Lipscomb, F. Baumann and W. Kaim, *Organometallics*, 1998, **17**, 293.
- T. Kotte and D. Stalke, *Angew. Chem., Int. Ed. Engl.*, 1993, **32**, 580.
- W. Clegg, M. R. J. Elsegood, S. J. Teat, C. Redshaw and V. C. Gibson, *J. Chem. Soc., Dalton Trans.*, 1998, 3037.
- A. L. Spek, PLATON, University of Utrecht, The Netherlands, 2000.
- SMART and SAINT software for CCD diffractometers, Bruker AXS Inc., Madison, WI, USA, 1997.
- G. M. Sheldrick, SHELXTL user manual, version 5.1, Bruker AXS Inc., Madison, WI, USA, 1997.